Distinct Molecular Motions in a Switchable Chromophore Dielectric 4-*N*,*N*-Dimethylamino-4′-*N*′-methylstilbazolium Trifluoromethanesulfonate

Zhihua Sun, Junhua Luo, Tianliang Chen, Lina Li, Ren-Gen Xiong, Ming-Liang Tong, and Maochun Hong*

Molecular motion associated with rotational and orientational phase transitions is one of the prominent structural strategies for assembling the functional materials such as artificial motors and tunable molecular dielectrics. Here, a new organic chromophore molecule, 4-*N*,*N*-dimethylamino-4′-*N*′-methylstilbazolium trifluoromethanesulfonate (complex 1), which undergoes an exceptional order-disorder phase transition at 322 K, is successfully synthesized. The single crystal X-ray diffraction analysis, thermal analysis, and dielectric measurements are used to characterize its dielectric dynamic behaviors. The results reveal that 1 behaves as a molecular rotator with the obviously distorted bipyramidal geometry of trifluoromethanesulfonate anions. In addition to its disorderings, two very distinct motions of the anionic moieties are confirmed, namely the "earth rotation" of partial units and the "earth revolution" of the whole molecule. Such unique molecular motions are found to be mainly responsible for the order–disorder phase transition together with the abrupt dielectric anomaly and anisotropy. The charge-transfer cationic parts enhance the molecular motions behaving as the stator and give rise to its excellent third-order nonlinearities. The concept may allow for the remote control of molecular events to explore functional materials in organic chromophores.

1. Introduction

Molecular motions associated with phase transition have been explored in a wide range of materials and may greatly affect their properties. Utilizing the exciting possibility of dynamic and related behavior caused by rotational or orientational motion, molecular rotator has been used to assemble the artificial molecular machines such as shuttles, brakes, tweezersand and potential molecular dielectrics.[1] Among them, dielectric switching complex has attracted great attentions for researchers, owing to the potential application in data communication, signal processing and sensing, and rewriteable optical data storage, etc.[2] Though much progress had been achieved in designing sophisticated small molecular analogue machines,[3] the major challenge is to regularly control the motions of the dipole moments with principle. One of the most promising strategies is to assemble complex functional materials that possess molecular-level properties and functions in a collective manner at the macroscopic scale.[4] For example, the 180° flip-flop molecular random motion of a rotatory unit could give rise to a rotation of the local structure, resulting in the formation of phase transition from high-temperature disordered state to low-temperature ordered state.[5] Unorientational motion of partial units within the range of ±30° was also observed during the ferroelectric phase transition.[5]

Recently, Collet et al. had discovered the novel ferroelectric structural order in the pure organic charge-transfer (CT) crystal at the molecular level.[6] Surprisingly, a series of configurational-locked polyene organic chromophores were synthesized with unique reversible phase transition from a low-temperature higher symmetry to the high-temperature lower symmetry.[7] As one of the most outstanding CT framework, hemicyanine dye of the stilbazolium chromophore was used to assemble potential ferroelectrics with above-room temperature phase transition.[8] However, to our knowledge, the microscopic mechanism of such phase transitions and the concomitant solid-solid structural transformations were not fully understood. Encouraged

Dr. Z. Sun, Prof. J. Luo, T. Chen, L. Li, Prof. M. Hong
Key Laboratory of Optoelectronic Materials
Chemistry and Physics
Fujian Institute of Research on the Structure of Matter
Chinese Academy of Sciences
Fuzhou, Fujian 350002, China
E-mail: jhluo@fjirsm.ac.cn

Prof. R.-G. Xiong
Ordered Matter Science Research Center
Southeast University
Nanjing 210096, China

Prof. M.-L. Tong
State Key Laboratory of Optoelectronic Materials and Technologies
School of Chemistry and Chemical Engineering
Sun Yat-Sen University
Guangzhou 510275, China

DOI: 10.1002/adfm.201201770

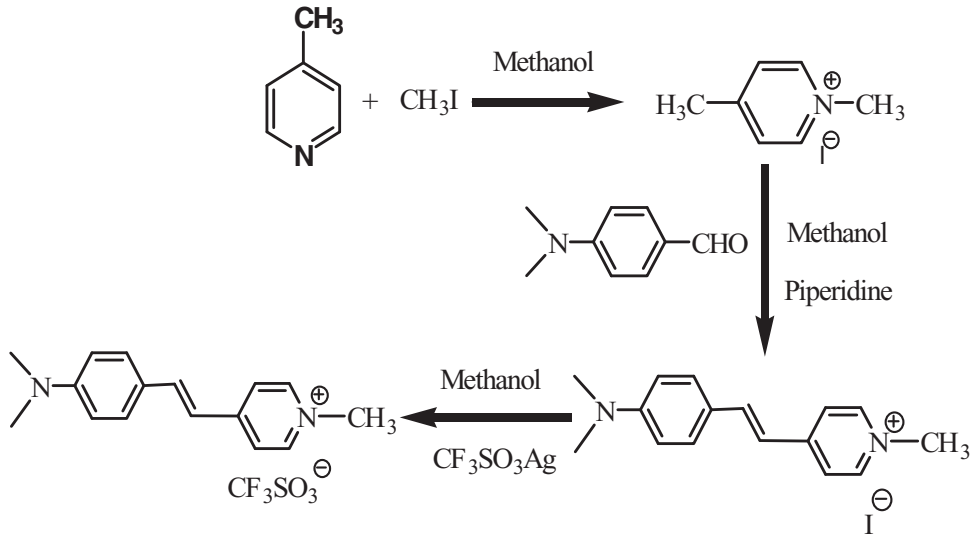

Scheme 1. The synthesis routine of **1**.

by the pioneering work, herein, we presented a new switchable molecular dielectric based on the CT stilbazolium chromophore, 4-*N*,*N*-dimethylamino-4′-*N*′-methylstilbazolium trifluoromethanesulfonate (complex **1**), with a reversible phase transition utilizing the molecular motion of trifluoromethanesulfonate anionic moiety. For **1**, its anion acts as a rotator while the chromophore cation behaves as the stator-like part during phase transition. With the enhanced stabilization of cation, exceptionally distinct mechanical motions of the anionic moieties were firstly observed, i.e., the "earth rotation" of partial units and the "earth revolution" of the whole molecule.

2. Results and Discussion

Complex **1** was synthesized by the ion-exchange reaction of trifluoromethanesulfonate silver and 4-*N*,*N*-dimethylamino-4′-*N*′-methylstilbazolium iodide, which was prepared from 4-picoline, methyl iodide and 4-*N*,*N*-dimethylamino-benzaldehyde in the presence of piperidine as catalyst (**Scheme 1**). Large-size crystals were successfully grown from the methanol solutions as the red plates perpendicular to the *c*-axis by the temperature lowing method (**Figure 1**). In the growth commencement, a saturated solution was hermetically kept at 5–6 °C above its saturated temperature for 24 h. With decreasing the solution temperature to its saturated status, the perfect seed-crystal obtained by the spontaneous nucleation was dipped into solution. Before crystal growth, the seed-crystal was maintained in the solution slightly above saturated status for homogenization. The temperature-lowering rate for crystal growth was 0.05 °C/day. The straightforward fabrication of bulk crystals with high optical qualities guarantees its potential device application. The purity of the as-grown crystals was confirmed by the IR spectrum, element analysis and X-ray powder diffraction matching with the single-crystal structural determination at room temperature (see Supporting Information Figure S1,S2).

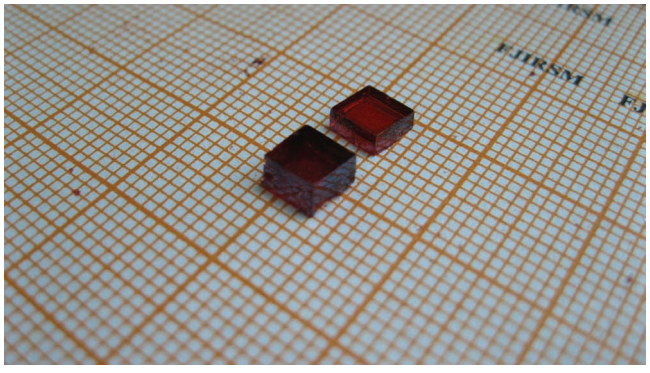

Figure 1. The as-grown crystals of 1 with the respective 3D sizes of 4.8 × 4.5 × 3.2 mm^3 and 4.1 × 4.0 × 2.6 mm^3.

Differential scanning calorimetry (DSC) measurement was used to detect phase transition and to confirm the existence of heat anomaly. As shown in **Figure 2**a, a sharp endothermic peak appearing at the phase transition temperature (T_c = 322 K) and the relative large heat hysteresis (≈6 K) were clearly recorded, which indicate that complex **1** undergoes a first-order phase transition.[9] Entropy change ΔS accompanying the transition was estimated as ≈6.4 J mol^{-1} K^{-1}. Given that $\Delta S = nR\ln N$, where R is the gas constant and N is the ratio of possible configurations in the disorder system, it obtains N = 2.1, which indicates the order–disorder transition undergoing reorientations at two sites.[10] Furthermore, the sharp heat capacity peak also corresponds well to the phase transition in the heating mode. From the specific heat *vs* temperature curve, the respective ΔS and N are approximately calculated as 6.56 and 2.2, coinciding fairly well with the DSC results and further confirming the typical order-disorder transition.

What greatly favors its potential application as the switchable molecular dielectric is that its melting temperature is far beyond T_c, approaching 484 K as shown in the thermal analysis curves (Figure 2b). Such a large temperature gradient (≈162 K) between phase transition and melting point makes **1** possess great advantage to be fabricated into the applicable device. For convenience, we label the phase at 343 K as the high-temperature phase (HTP), the phase at 293 K as the room-temperature

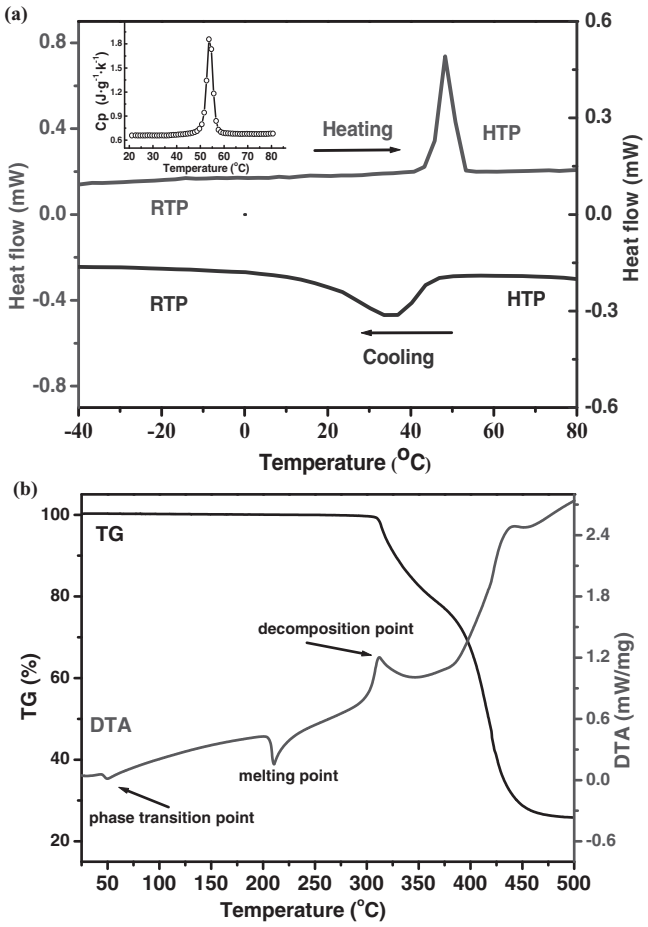

Figure 2. DSC measurements obtained on a heating-cooling cycle (a) and the TG/DTA curves of 1 with heating rate 10 °C/min (b). Temperature dependence of the specific heat (Cp) deduced from DSC data in the heating mode is shown in the inset of (a).

phase (RTP). Crystal structures were also resolved at 338 K (ITP) and 93 K (LTP) for forthcoming comparative investigation.[11] Variable-temperature X-ray single-crystal diffraction reveals that **1** crystallizes in the centrosymmetric space group $P2_1/c$ in RTP with cell parameters of a = 17.508(5), b = 7.607(2), c = 13.533(4) Å, β = 93.712(6)° and V = 1798.4(10) Å^3. As to LTP structure, it adopts the same structure as that in RTP and little difference can be seen by comparing the crystal data, suggesting that there is no occurrence of phase transition between 293 and 93 K. However, what interests us is the crystallographic transformation from RTP to HTP. Though its HTP still belongs to $P2_1/c$ space group, β becomes to 90.05° almost possessing the orthorhombic feature, and the detailed cell parameters are a = 7.190(9), b = 7.698(10), c = 34.08(4) Å and V = 1886(4) Å^3. Except for the consensus of b-axis length, all the values of a-, c-axis lengths and β angle change markedly owing to the phase transition. According to the traditional phase transition theory, the RTP structure usually adopts a subgroup of HTP, namely the HTP for **1** should be determined in an orthorhombic system with higher symmetry operations. However, its structure still persists in the monoclinic system even the temperature increases far away from the critical point, which is also confirmed from the variable-temperature XRPD patterns. Thus, it is difficult to describe the phase transition with a proper Aizu notion. Using Landau's phenomenological approach,[12] the metastable phases may coexist with the parent phase in the first-order phase transition arousing a thermal hysteresis. Perhaps, HTP for **1** is such a metastable phase even far away from the critical point.

Figure 3a shows the molecular crystal structures of **1** at RTP and HTP. In the organic cation, the main part of π-conjugated bridge from $(CH_3)_2N$- group to pyridinium acceptor exhibits as a planar mirror.[13] The striking feature of its packing is that the polar polymer-like cations are stacked up along the b-axis, and anions link them together utilizing weak hydrogen bonds (Supporting Information Figure S3). As checked by PLATON, C−H···O hydrogen bonds are the main molecular interactions in addition to the van der Waals force. Oxygens of $CF_3SO_3^-$ anions are involved in bifurcated hydrogen bonds acting as the acceptor. One direction corresponds to $C_5H_4N-CH_3\cdots O_2$ group and the other links carbon atom of pyridine ring. At room temperature, the trifluoromethanesulfonate anions exhibit almost ordered and ideal tetrahedral geometry of bipyramidal. Contrarily, symmetry of both pyramidals is broken upon higher temperature, revealing the existence of a highly disordered anion. Thus, the phase transition is confirmed as an order-disorder type, matching very well with the crystallographic data and DSC results.

In order to further confirm the above-mentioned phase transition, variable-temperature X-ray powder diffraction was performed on the polycrystalline samples of **1**. The comparative spectra (**Figure 4**) indicate that the phase transition occurs above 322 K. All the diffraction patterns coincide fairly well with the simulated ones at different temperatures (Supporting Information Figure S2).

Severe changes of physical properties approaching critical point could also support the phase transition. Here, dielectric experiments of the complex relative permittivity were performed on crystal samples of **1**. All the faces were selected in accordance with the RTP structure. In the heating mode, both the dielectric constants and loss along all the directions keep stable until the temperature reaches 322 K (**Figure 5**). Subsequently, the permittivity exhibits an obvious increase followed by a clear slope and then remains almost constant, indicating the appearance of phase transition. What interests us is the existence of a tiny dielectric relaxation process at different frequencies, indicating a relatively slow dipolar motion of the huge organic molecule of **1**. Similarities have been examined for some other stilbazolium compounds.[8] Macroscopic relaxation time was roughly estimated from the frequency dependence of ε' at the inflection point of the curves. For a Debye peak, the condition for the peak is $2\pi\tau f = 1$ and the detailed relationship can be described by the Arrhenius equation, $\ln f = -\ln(2\pi\tau_o) - E_a/RT$, where T is the temperature and f is the vibration frequency. Thus, the activity energy E_a and relaxation time τ_o can be estimated according to the experimental data of $\ln f$ *vs* 1/T. The average E_a and τ_o for **1** are approximately calculated to be 96 kJ/mol and 1.5 $\times 10^{-4.5}$ s, respectively. The magnitude value of E_a is similar to that of other compounds (usual value ≈10 to 70 kJ/mol).[14] The cooperative motions and the steric

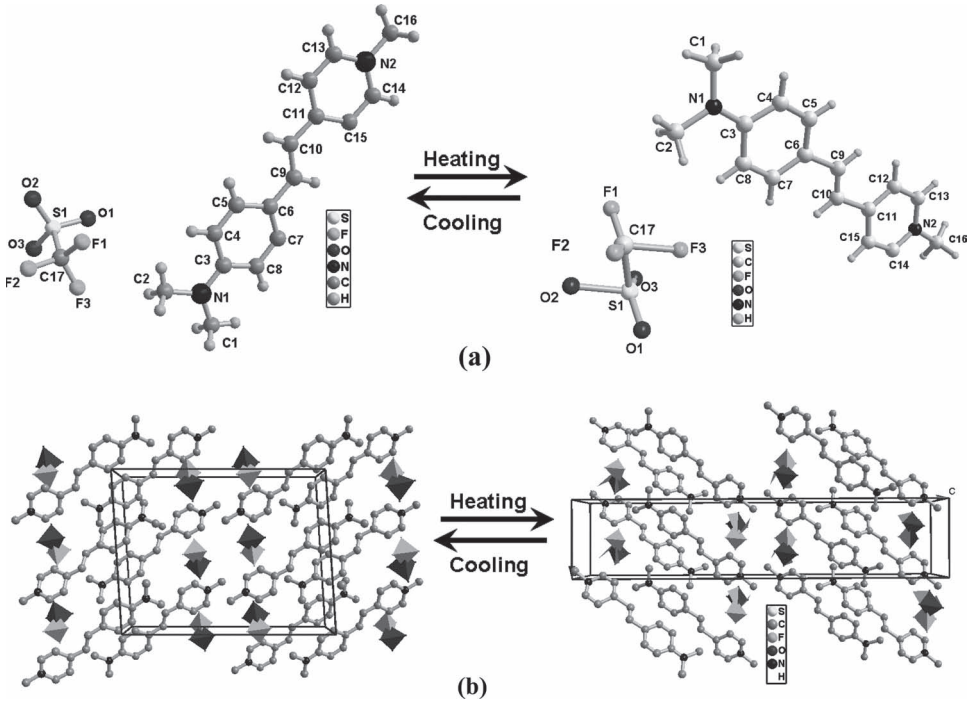

Figure 3. The molecular units of 1 in RTP and HTP with the trifluoromethanesulfonate anion disordered in the HTP (a). The packing structures are viewed along the *b*-axis with the phase transition from RTP to HTP (b). Symmetry breaking occurs in the ordered and ideal bipyramidal of trifluoromethanesulfonate anion, originating from the reversible phase transition.

hindrance of huge organic molecules for **1** might contribute to slightly higher activity energy.

In addition, the dielectric permittivities of **1** present a striking anisotropy along the different crystallographic axes. In the HTP, values of dielectric permittivity at 5 KHz along [001] direction are three- and four-times larger than those along [020] and [–100] directions respectively, while the corresponding values in RTP allow for the dielectric anisotropy of $\varepsilon'_c/\varepsilon'_b = 4.2$ and $\varepsilon'_c/\varepsilon'_a = 3.8$. To our best knowledge, such a large temperature-independent dielectric anisotropic behavior is rarely reported in the pure organic complex. Furthermore, a stronger anomaly was observed in the *c*-axis direction, compared with a smaller one recorded along the two-fold axis direction. Xiong et al. qualitatively explained the dielectric anisotropy of a nickel(II) complex.[15] Herein, we propose that such a strong dielectric anisotropy mainly depend on the intrinsic structural diversification upon high temperature. It can be seen from the crystal structures that *c*-axis length exhibits an extremely larger variety than both *a*-axis and *b*-axis with the increasing temperature, which clearly shows that *c*-axis is much more sensitive to the external stimuli especially at low frequency, in good agreement with switchable dielectric character. Otherwise, the planar organic cation lies almost perpendicular to the *b*-axis in the RTP. Considering the equivalent effect induced by the anions, the unidirectional CT in the organic plane will yield smaller dipole-moment along the *b*-axis, hence leading to less change of dielectric permittivity in this direction. The

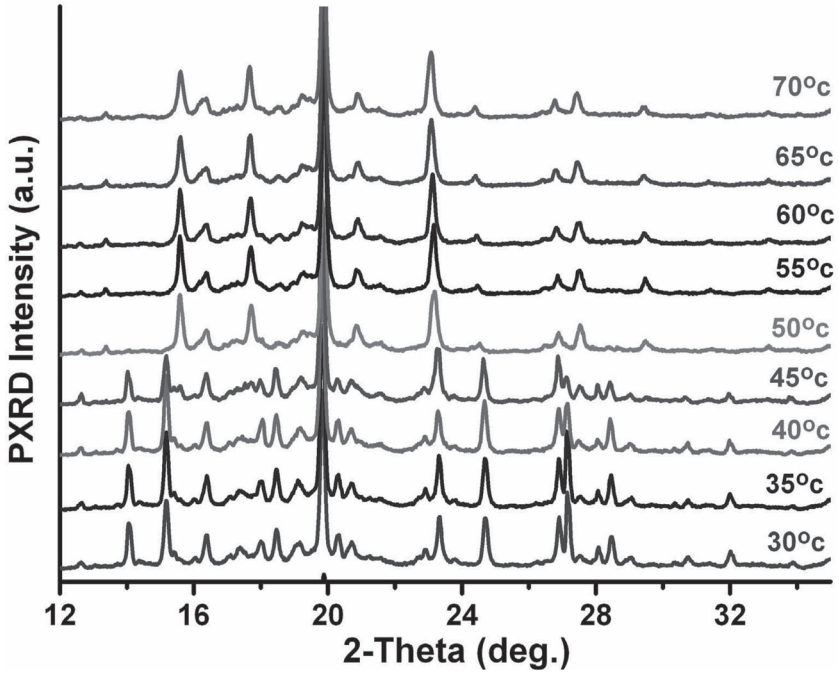

Figure 4. The variable-temperature X-ray powder diffraction patterns of **1**.

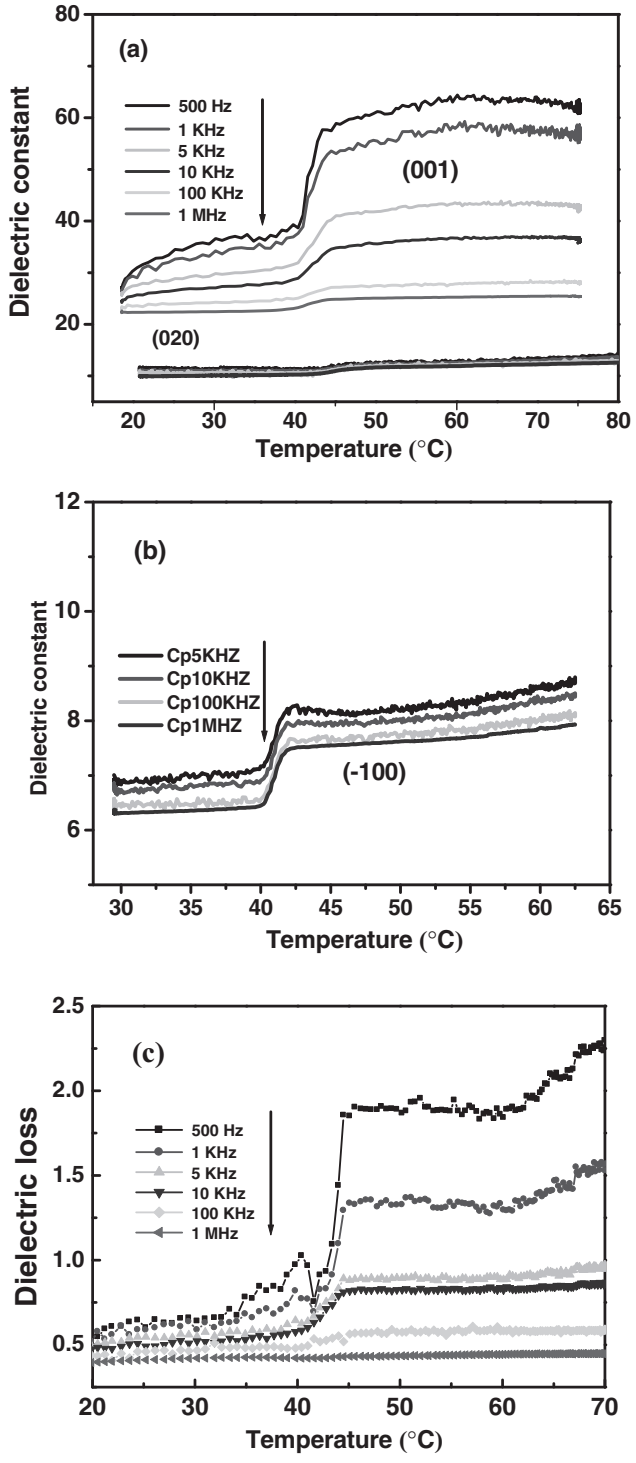

Figure 5. a,b) Temperature-dependent dielectric constants of **1** on crystal samples along the different crystallographic directions of (001), (020), and (-100). The dielectric loss as the function of temperature along (001) direction is presented in (c).

variation of permittivities along the direction perpendicular to molecular plane matches well with dielectric behaviors of some substances with free- and frozen-rotator phases.[16]

To obtain further insights into the microscopic origin of the phase transition for **1**, its structural transformation of anionic moieties was shown in **Figure 6**, together with the temperature dependence of theoretical order parameter. In the RTP, all the F atoms in the anion occupy the pyramidal vertex with equivalent C−F bonds (≈1.3 Å) and F−C−F angles (≈107°), suggesting the existence of an ordered pyramidal. Similarly, the O atoms also locate harmoniously in the other pyramidal (Supporting Information Table S1). Thus, the trifluoromethanesulfonate anion exhibits the ordered and ideal tetrahedral geometry of bipyramidal. With the temperature increasing into HTP, the symmetry-breaking occurs accompanied with the disequilibrium of C−F and S−O bonds. As the arrows indicate, both contraction and elongation of bonds occur and distort the ideal pyramidal, constructing a highly disordered anion. The sharp decline of order parameter approaching T_c would also strongly support the order-disorder phase transition.[17] In addition to the dynamical disorderings, another strikingly interesting feature is to observe two distinct types of molecular motions of the anionic moiety, i.e., the earth rotation of partial units around S_1-C_{17} bond and the earth revolution of the whole molecule. As shown in **Figure 7**, the $-SO_3$ polyhedron rotates anticlockwise while–CF_3 polyhedron behaves in the clockwise rotation. Such a motion is described like the earth rotation, which is supported by the detailed data of F−C−F and O−S−O angels in Table S1 (Supporting Information). Meanwhile, the anionic moiety also revolves referring to the cation plane which is an excellent D-$\pi\cdots$A planar CT chromophoric framework. When temperature increases, the $-SO_3$ tetrahedron falls towards the plane while the –CF_3 polyhedron uplifts away from the plane, resulting in the orientational motion of the whole molecule. Namely, the stilbazolium cation functions as a stator which favors to the motions of anion-rotator. The included angle between S_1-C_{17} line and cation plane would clearly depict such a motion like the earth revolution. In LTP, the included angle is calculated as 60.5° between the rotation axis and cation plane, while the corresponding value becomes 9.3° in HTP. Hence, the 51.2° orientational motion of anionic moiety occurs, leading to the macroscopic phase transition together with the structural distortion. As we are aware, this is the first observation of such interesting motions triggered by the increasing temperature during the phase transition.

The comparative structure analysis indicates the cationic moiety seems to make no contribution to the phase transition. However, the weak hydrogen bonds are sensitive to heat and may have a significant impact on its properties.[18] For example, the distance of C_{14}-H$\cdots O_2$ changes from 3.178 Å to 3.338 Å when comparing its RTP and HTP. This thermal-induced elongation effect may also response for the activation of molecular freedom degree or order parameter, because it generates an increase in the ionic displacement similar to other compounds.[19] Most probably, the weakness of hydrogen-bonded interaction favors the anionic rotation and enhances the cationic CT process. Here, ab initio calculations at RHF/3-21G* level show that molecular HOMOs mainly localize in 4-*N*-styryl while LUMOs in cationic pyridinium ring and the bridge, giving a significant charge displacement from benzenium to pyridinium-ring (see Supporting Information Figure S4-S6). The HOMO-LUMO energy gap ΔE_{HL} is theoretically estimated

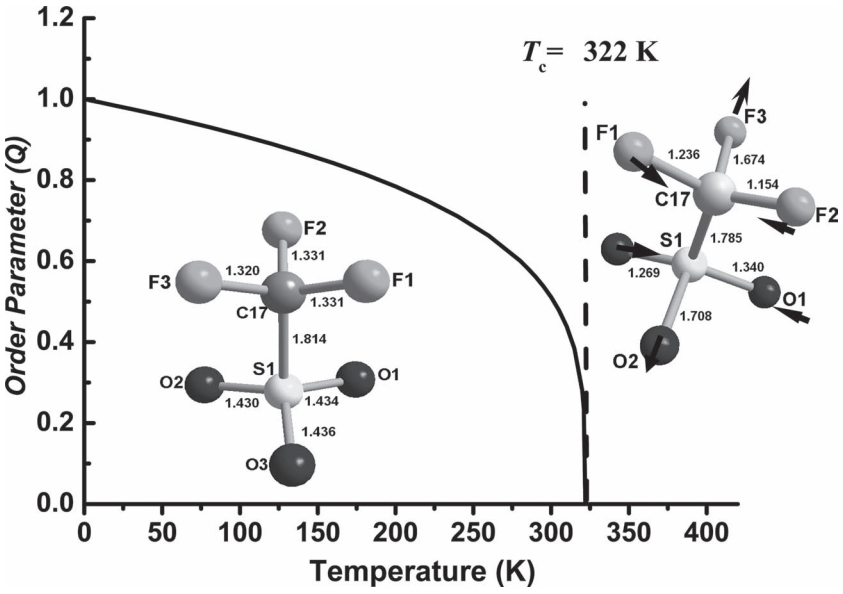

Figure 6. Dynamical order–disorder transformation of anionic moieties at RTP and HTP with the temperature dependence of theoretical order parameter (Q). RTP shows the ordered and ideal tetrahedral geometry of bipyramidal, while the symmetry-breaking occurs in HTP.

to be 5.032 eV, much larger than experimental result from its absorption spectra. Experimental Z-scan reveals a strong NLO absorption, regarded as saturable absorption. The NLO refractive index (n_2) and absorption coefficient (β) were respectively determined as 1.585×10^{-19} m^2/W and -2.621×10^{-12} m/W. The modulus of effective third-order susceptibility $\chi^{(3)}$ and second molecular hyperpolarizability γ are calculated as 5.086×10^{-13} esu and 3.998×10^{-31} esu (Supporting Information Table S2), revealing its potential application as a third-order NLO candidate.

3. Conclusion

In conclusion, the present work has successfully demonstrated a new switchable molecular dielectric, which undergoes an exceptional order-disorder phase transition at 322 K. The distorted trifluoromethanesulfonate anion behaves as the molecular-rotator while the chromophore cation acts as the stator-like part. Besides the disorderings, two exceptionally distinct molecular motions were observed in the anionic moieties, namely the earth rotation of partial units and the earth revolution of the whole molecule. Above the critical point, the anionic moiety exhibits an unprecedented 51.2° orientational motion together with the structural distortion. The present work has revealed a previously undescribed feature of molecular motions and we believe the findings will urge exploration for new multifunctional materials in organic chromophores.

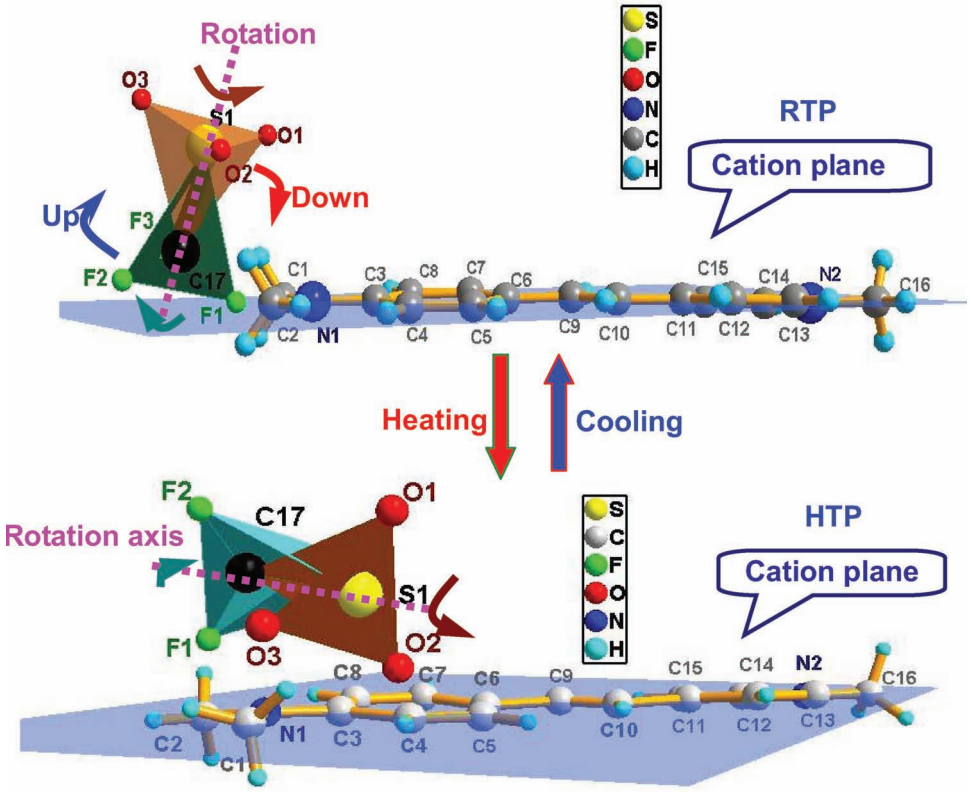

Figure 7. Schematic illustration of the exceptionally distinct molecular motions triggered with the phase transition. The cation plane acts as a stator-like part while the anionic moiety behaves as a rotator.

4. Experimental Section

All the chemical reagents were purchased as high purity (AR grade) and used without any further purification. The obtained salts for crystal growth were verified by element analysis, X-ray powder diffraction and FT-IR spectrum. FT-IR spectra were recorded on a Spectrum One spectrophotometer (PerkinElmer) using KBr pallets. XRPD patterns were recorded by an X-ray diffractometer (Rigaku Corporation SCXmini). Elemental analyses for C, H, N and O contents were performed on the Elementar Vario MICRO elemental analyzer. Anal. Calcd: H 4.93, C 52.57, N 7.21, O 12.36; found: H 4.89, C 52.60, N 7.20, O 12.33. Thermal stabilities and specific heat were respectively measured by TGA using a Netzsch STA 449C unit, and DSC using a differential thermal analyzer of Netzsch DSC 200 F3 with the heating rate of 10 K/min. Dielectric experiments were carried out on single-crystal specimen by TH2828 Precision LCR Meter. The electrodes were made by sputtering silver onto both sides of samples and attaching copper leads with silver paste. Calibration of standard capacitor reveals that the experimental errors are within ±3% accuracy. Third-order NLO properties were investigated using a picosecond laser (PY61C-10, Continuum, 532 nm at 28 ps) by the Z-scan technique.

All the crystal structures of **1** were measured on Rigaku CCD diffractometer with Mok_α radiation (λ = 0.71073 Å) at various temperatures. The CrystalClear software package (Rigaku, 2005) was used for data collection, cell refinement and data reduction. Crystal structures were solved by the direct methods and then refined by the full-matrix method based on F^2 using the SHELXTL software package (Sheldrick, 2008). All non-hydrogen atoms were located from the trial structure and refined anisotropically with SHELXTL using the full-matrix least-squares procedure. The positions of hydrogen atoms were generated geometrically and allowed to ride on the parent atoms.

Supporting Information

Supporting Information is available from the Wiley Online Library or from the author.

Acknowledgements

This work was financially supported by the NSFC (Nos. 51102231 and 21171166), the 973 Key Programs of the MOST (Nos. 2010CB933501 and 2011CB935904) the One Hundred Talent Program of Chinese Academy of Sciences, and the Key Project of Fujian Province (2012H0045).

Received: June 28, 2012
Published online: July 26, 2012

[1] a) Z. Dominguez, T.-A. Khuong, H. Dang, C. N. Sanrame, J. E. Nuñez, M. A. Garcia-Garibay, *J. Am. Chem. Soc.* **2003**, *125*, 8827; b) M. A. Garcia-Garibay, *Proc. Natl. Acad. Sci. USA* **2005**, *102*, 10771; c) T. Akutagawa, H. Koshinak, D. Sato, S. Takeda, S. Noro, H. Takahashi, R. Kumai, Y. Tokura, T. Nakamura, *Nat. Mater.* **2009**, *8*, 342; d) K. Kinbara, T. Aida, *Chem. Rev.* **2005**, *105*, 1377; e) C. Lemouchi, C. S. Vogelsberg, L. Zorina, S. Simonov, P. Batail, S. Brown, M. A. Garcia-Garibay, *J. Am. Chem. Soc.* **2011**, *133*, 6371; f) J. D. Badjić, V. Balzani, A. Credi, S. Silvi, J. F. Stoddart, *Science* **2004**, *303*, 1845; g) D. A. Leigh, J. K. Wong, F. Dehez, F. Zerbetto, *Nature* **2003**, *424*, 174.

[2] a) M. Wuttig, N. Yamada, *Nat. Mater.* **2007**, *6*, 824; b) M. Salinga, M. Wuttig, *Science* **2011**, *332*, 543; c) D. Lencer, M. Salinga, M. Wuttig, *Adv. Mater.* **2011**, *23*, 2030; d) H. Zheng, J. B. Rivest, T. A. Miller, B. Sadtler, A. Lindenberg, M. F. Toney, L.-W. Wang, C. Kisielowski, A. P. Alivisatos, *Science* **2011**, *333*, 206.

[3] a) T. Muraoka, K. Kinbara, Y. Kobayashi, T. Aida, *J. Am. Chem. Soc.* **2003**, *125*, 5612; b) T. Muraoka, K. Kinbara, T. Aida, *Nature* **2006**, *440*, 512; c) V. Serreli, C. F. Lee, E. R. Kay, D. A. Leigh, *Nature* **2007**, *445*, 523; d) J. V. Hernández, E. R. Kay, D. A. Leigh, *Science* **2004**, *306*, 1532; e) S. P. Fletcher, F. Dumur, M. M. Pollard, B. L. Feringa, *Science* **2005**, *310*, 80.

[4] a) M. A. Garcia-Garibay, *Nat. Mater.* **2008**, *7*, 431; b) H. Kitagawa, Y. Kobori, M. Yamanaka, K. Yoza, K. Kobayashi, *Proc. Natl. Acad. Sci. USA* **2009**, *106*, 10444; c) C. S. Vogelsberg, M. A. Garcia-Garibay, *Chem. Soc. Rev.* **2012**, *41*, 1892.

[5] D.-W. Fu, W. Zhang, H.-L. Cai, Y. Zhang, J.-Z. Ge, R.-G. Xiong, S. D. Huang, *J. Am. Chem. Soc.* **2011**, *133*, 12780.

[6] E. Collet, M. L. Cailleau, M. B.-L. Cointe, H. Cailleau, M. Wulff, T. Luty, S.-Y. Koshihara, M. Meyer, L. Toupet, P. Rabiller, S. Techert, *Science* **2003**, *300*, 612.

[7] O.-P. Kwon, S.-J. Kwon, M. Jazbinsek, A. Choubey, V. Gramlichs, P. Günter, *Adv. Funct. Mater.* **2007**, *17*, 1750.

[8] G. Xu, Y. Li, W.-W. Zhou, G.-J. Wang, X.-F. Long, L.-Z. Cai, M.-S. Wang, G.-C. Guo, J.-S. Huang, G. Batorb, R. Jakubas, *J. Mater. Chem.* **2009**, *19*, 2179.

[9] a) D. W. Fu, W. Zhang, H.-L. Cai, J.-Z. Ge, Y. Zhang, R. G. Xiong, *Adv. Mater.* **2011**, *23*, 5658; b) J. Z. Ge, X. Q. Fu, T. Hang, Q. Ye, R. G. Xiong, *Cryst. Growth Des.* **2010**, *10*, 3632; c) W. Zhang, Y. Cai, R. G. Xiong, H. Yoshikawa, K. Awaga, *Angew. Chem. Int. Ed.* **2010**, *49*, 6608.

[10] a) Z. Sun, T. Chen, J. Luo, M. Hong, *Angew. Chem., Int. Ed.* **2012**, *51*, 3871; b) H.-L. Cai, W. Zhang, J.-Z. Ge, Y. Zhang, K. Awaga, T. Nakamura, R.-G. Xiong, *Phys. Rev. Lett.* **2011**, *107*, 147601.

[11] Crystal data for complex **1** at 93 K (**LTP**): a = 17.500(12), b = 7.605(5), c = 13.547(9) Å, β = 93.708(13)°, V = 1799(2) Å^3, Z = 4, ρ_{calcd} = 1.434 g/cm^3, $R_1(I > 2\sigma(I))$ = 0.0578, $wR_2(I > 2\sigma(I))$ = 0.1230, S = 1.145; **1** at 293 K (**RTP**): $C_{17}H_{19}F_3N_2O_3S$, M_r = 388.40, Monoclinic, $P2_1/c$, a = 17.508(5), b = 7.607(2), c = 13.533(4) Å, β = 93.712(6)°, V = 1798.4(10) Å^3, Z = 4, ρ_{calcd} = 1.401 g/cm^3, $R_1(I > 2\sigma(I))$ = 0.0575, $wR_2(I > 2\sigma(I))$ = 0.1687, S = 0.979; **1** at 338 K (**ITP**): a = 7.1842(14), b = 7.6856(17), c = 34.011(7) Å, β = 90.111(4)°, V = 1877.9(7) Å^3, ρ_{calcd} = 1.374 g/cm^3, $R_1(I > 2\sigma(I))$ = 0.1085, $wR_2(I > 2\sigma(I))$ = 0.3188, S = 1.102; **1** at 343 K (**HTP**): a = 7.190(9), b = 7.698(10), c = 34.08(4) Å, β = 90.05(4)°, V = 1886(4) Å^3, Z = 4, ρ_{calcd} = 1.368 g/cm^3, $R_1(I > 2\sigma(I))$ = 0.1027, $wR_2(I > 2\sigma(I))$ = 0.2304, S = 0.838. CCDC 865587-865590 contain the supplementary crystallographic data, which can be obtained free of charge from Cambridge Crystallographic Data Center via www.ccdc.cam.ac.uk/data_request/cif.

[12] C. Cayron, *TEM study of interfacial reactions and precipitation mechanisms in Al_2O short fiber or high volume fraction SiC particle reinforced Al-4Cu-1Mg-0.5Ag squeeze-cast*, Chapter 5, *Introduction to Order-Disorder Transitions*. Ph. D thesis, Lausanne, EPFL 2000.

[13] a) Y. C. Shu, Z. H. Gong, C. F. Shu, E. M. Breitung, R. J. McMahon, G. H. Lee, A. K.-Y. Jen, *Chem. Mater.* **1999**, *11*, 1628; b) K. Staub, G. A. Levina, S. Barlow, T. C. Kowalczyk, H. S. Lackritz, M. Barzoukas, A. Fort, S. R. Marder, *J. Mater. Chem.* **2003**, *13*, 825.

[14] X.-L. Li, K. Chen, Y. Liu, Z.-X. Wang, T.-W. Wang, J.-L. Zuo, Y.-Z. Li, Y. Wang, J. S. Zhu, J.-M. Liu, Y. Song, X.-Z. You, *Angew. Chem. Int. Ed.* **2007**, *46*, 6820.

[15] D.-W. Fu, Y.-M. Song, G.-X. Wang, Q. Ye, R.-G. Xiong, T. Akutagawa, T. Nakamura, P. W. Chan, S. D. Huang, *J. Am. Chem. Soc.* **2007**, *129*, 5346.

[16] a) T. Akutagawa, H. Koshinaka, D. Sato, S. Takeda, S.-I. Noro, H. Takahashi, R. Kumai, Y. Tokura, T. Nakamura, *Nat. Mater.* **2009**, *8*, 342; b) E. Laukhina, J. V. Gancedo, S. Khasanov, V. Tkacheva, L. Zorina, R. Shibaeva, J. Singleton, R. Wojciechowski, J. Ulanski, V. Laukhin, J. Veciana, C. Rovira, *Adv. Mater.* **2000**, *12*, 1205.

[17] S. A. T. Redfern, E. Salje, A. Navrotsky, *Contrib. Mineral Petrol.* **1989**, *101*, 479.

[18] a) A. Kozak, M. Grottel, A. E. Kozioz, Z. Pajak, *J. Phys. C: Solid State Phys.* **1987**, 5433; b) M. Szafrański, *J. Phys. Chem. B* **2011**, *115*, 8755.

[19] a) S. Gima, Y. Furukawa, D. Nakamura, *Ber. Bunsen. Ges.* **1984**, *88*, 939; b) O. Czupiński, M. Wojtaś, J. Zaleski, R. Jakubas, W. Medycki, *J. Phys.: Condens. Matter* **2006**, *18*, 3307.